

# The influence of the edge characteristics of detected objects on underwater active electrolocation system

Yingli Wang, Jiegang Peng\*, Lu Liu

*School of Automation Engineering and Center for Robotics, University of Electronic Science and Technology of China, Chengdu, 610054, People's Republic of China*

DOI: 10.5185/amlett.2018.7111

www.vbripress.com/aml

## Abstract

The active electrolocation technology has been developed for near 60 years and played a significant role in the field of biomimetic sensor. But the influence of the edge characteristics of detected objects on underwater active electrolocation system was rarely investigated. In this paper, an experiment system based on the underwater active electrolocation technology is built. The amplitude information-frequency characteristics (AIFC) for different probed objects with the different edge characteristic and approximate volumes are investigated. Two sets of different edge characteristic shapes (cylinder and cuboid, cone and pyramid), whose volumes are little difference in each sets, are carried out in the same materials to deeply study on the effect. The height variation curve (HVC) is employed to compute the frequency inflection point (FIP) of AIFC for the system. According to experiment results, we find that the FIP for the probed metallic objects with similar volumes is weighty associated to the edge characteristics of objects, while the FIP for the plastic has nothing to do with the edge characteristics of objects. It may have reference value for physical mechanism of weakly electrical fish active electrolocation system. Copyright © 2018 VBRI Press.

**Keywords:** Object edge characteristic, Amplitude Information-Frequency Characteristics (AIFC), height variation curve (HVC), active electrolocation, Frequency Inflection Point (FIP).

## Introduction

In South America, some weakly electric fish, e.g. Gymnotiformes, have the ability that it can detect objects and orientation in a completely dark environment through the way perceiving the changes of the surrounding electric field by their electric organ [1]. Inspired by the ability, an innovation for the sensor technology, active electrolocation technology, was generated and gains much attention for a long time. Since biologist found that much information (distance, location, size and shape) can be obtained by the weakly electric fish, the active electrolocation technology has been studied extensively and played an important role in the field of biosensors [2]-[5]. In 1996, B. Rasnow perfected the mathematical model for active electrolocation of weakly electric fish based on the work of others [6]. In 1998, Australia researchers, Chetty G and Russell A, invented an underwater robot imitating the ability of the weakly electric fish, which can realize the function of avoiding obstacles [7]. In 2011, Michael D. Freezor designed an underwater vehicle that can perform the underwater navigation and positioning [8]. In 2012, the investigation of M. G. Metzén illustrates that active electrolocation technology has an important role in detecting the vulnerable plaque which is considered as one of factors causing arteriosclerosis [9]. In 2015, the detect Frequency Dead Zone (DFDZ) and the Frequency

Inflection Point (FIP) of the amplitude information-frequency characteristics (AIFC) for the underwater active electrolocation system are found [10]. The DFDZ is a frequencies range of excitation signals, in which the electrolocation system cannot realize the location of object by using the AIFC. The FIP for the electrolocation system is the frequency of DFDZ at the moment.

Although the active electrolocation technology has been studied by researchers for near 60 years, there are a few studies on the influence of the edge characteristics of detected objects on the underwater active electrolocation system. In [11], Yang Bai has proposed that phase information is also influenced by geometry characteristics of object and distance of target. However their paper concerns the capacitive sensing component of electrosense. It has been proposed in [10] that the amplitude information-frequency characteristics (AIFC) of the underwater active electrolocation system have relevance to the material properties, geometric features of the detected object and conductivity of surrounding water, but the geometric volumes of the detected objects differ greatly. In addition, it is blurry the detail of relationship between AIFC and geometric properties of objects due to complicated underwater environment. To sum up, there are a few studies on the influence of the probed objects with the similar geometric features on the AIFC of the active electrolocation system.

In this study, the height variation curve (HVC) is proposed to study approximate volume of probed object with different edge characteristics such as approximate volume of cylinder and cuboid object how to influence on AIFC of the active electrolocation system. In order to investigate the influence, two sets of different shapes (cylinder and cuboid, cone and pyramid), whose volumes are little difference in each sets, will be selected for the active electrolocation system experiment.

**Methods and Experiment**

*Principle analysis*

In order to analysis the physical mechanism of weakly electrical fish active electrolocation system, a simple model composing of a pair of electric dipole source is designed shown in Fig. 1. When an object enters the electric field of the dipole, the distortion of electric field line will occur based on the difference between the properties of objects and the surrounding environment which can interfere with the electric field.

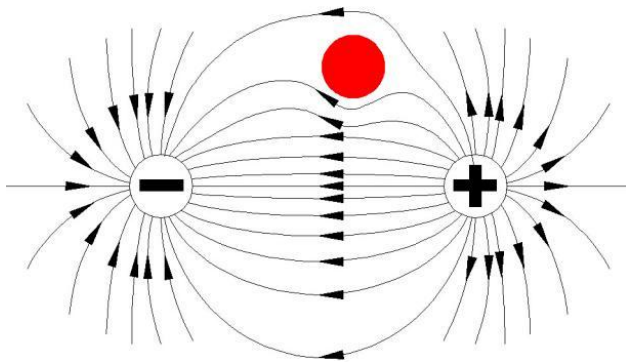


Fig.1. the distribution of electric field lines in a dipole with a object.

The interference is mainly manifested in the amplitude information-frequency characteristics of the electric field. The expression for the amplitude is shown as

$$\phi(\mathbf{r}) = E_0 \cdot \mathbf{r} \left( \frac{r_1}{r} \right)^3 \frac{\sigma_2 - \sigma_1 + i\omega(\epsilon_2 + \epsilon_1)}{2\sigma_1 + \sigma_2 + i\omega(2\epsilon_1 + \epsilon_2)} \quad (1)$$

where  $E_0$  is the electric field without disturbance,  $r=|\mathbf{r}|$  is the distance from the center of detected objects to the received signal point,  $\omega=2\pi f$  is the angular frequency of the excitation signal,  $\sigma_1$  and  $\sigma_2$  are the conductivity of the surrounding environment and objects,  $\epsilon_1$  and  $\epsilon_2$  are the dielectric constant of their, respectively. As can be observed from the formula (1), the amplitude is related to the resistivity and dielectric constant of the object and surrounding environment, the position of the object in the electric field, the size of the object.

In Error! Reference source not found., DFDZ and FIP of AIFC for the electrolocation system are attributed to the induced polarization (IP). The resistance for the underwater object is mutative based on the different frequencies due to the IP. According to the Cole-Cole model in 12, the expression for the impedance of the underwater object as

$$Z(i\omega) = R_0 \left[ 1 - m \left( 1 - \frac{1}{1 + (i\omega\tau)^c} \right) \right] \quad (2)$$

where the resistance  $R_0$  simulates unblocked pore paths by allowing parallel conduction through a purely resistive element, the  $m$  is the chargeability, theris the time constant and the  $c$  is the frequency dependence.

In general, conductivity of surrounding water have the certain influence on the parameter $\tau$ , the material properties of the underwater object have the certain influence on the parameter  $m$ . We speculate that the shape of the underwater object has the certain influence on the parameter  $\tau$ . So the resistivity of the underwater object whose possess different shapes and similar geometric features may be quite different based on the equation (2). The resistivity changes will cause the changes of FIP. In order to prove the guesses, in this paper, some controlled experiments about the guesses were made.

*Experiment introduction*

The electrolocation experiment apparatus shown in Fig. 2 (a) is built to simulate the weakly electric fish. It is composed of a computer, an NI-USB6289 data acquisition (DAQ) board, an interface panel, an electrode holder with emitting electrodes and receiving electrodes, two stepping motors and a water tank.

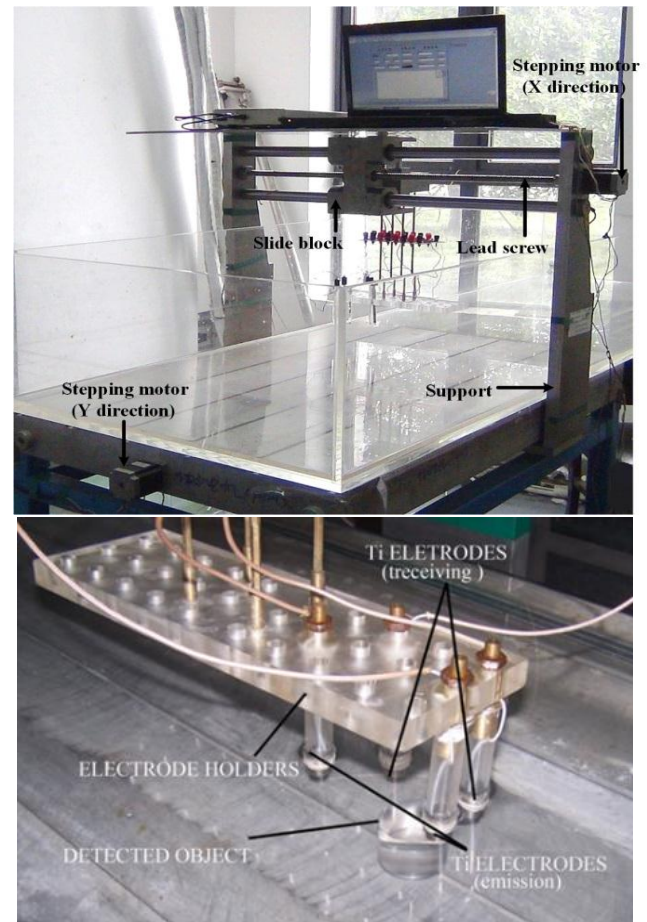


Fig.2. The underwater active electrolocation experimental apparatus.

The water tank used in this study had an internal dimension of  $1.80\text{m} \times 0.75\text{m} \times 0.40\text{m}$ . The artificial water poured in tank has a conductivity of  $340\ \mu\text{S}/\text{cm}$  at ambient temperature (around  $22^\circ\text{C}$ ). A total of 4 titanium electrodes were installed inside the tank in two lines (two emitting electrodes which is used to simulate the electric organ of the weakly electric fish and generate an electric field in the water and two receiving electrodes which is used to simulate the electric receptors in the skin of the weakly electric fish), attached to an electrode holder that was affixed to the slide block of lead screw shown in **Fig. 2(b)**. Only a bottom part of each electrode has contact with the water and the rest of it was wrapped with a cylindrical plexiglas sealing the gap with nonconductive epoxy. The distance between two emitting electrodes was  $0.09\text{m}$  and the distance between two receiving electrodes was  $0.06\text{m}$ . The electrode holder moved from left to right along the X-axis direction and the slide block of lead screw moved along the Y-axis direction with the rotation of two stepping motors. The host computer controls two stepping motors by controlling counters of NI-USB6289. In the experiments, the trajectory of the detection processes is a straight line paralleled to X-axis. The object was located in mid position of the trajectory. The velocity of the electrode holder was set  $3\text{mm s}^{-1}$  to insure enough sampling points of each waveform. The excitation source is a sinusoidal signal with  $2\text{V}$  peak-to-peak amplitude.

#### Acquisition and processing of data

The analog inputs of emitting electrodes and data acquisition of receiving electrodes were achieved by the computer through controlling the NI-USB6289. The detection signal ~ time curves for whole detection processes are shown in **Fig. 3 (a)**. Its X-axis position can be considered as the position of the electrode holder in the whole detection processes due to the constant velocity of it, Y-axis is the potential output of the detection signal. When the electrode holder close to the object, the amplitude of detection signal potential output will gradually decrease. Instead, the amplitude of detection signal potential output will gradually increase if the electrode holder far away to the object.

The curve consisting of all peak points of the detection signal ~ time curves is shown in **Fig. 3 (b)**. In order to show the amplitude and analyze the FIP better, we defined that the height variation curve (HVC) is the value  $h$  of the crest or trough minus the common shown in **Fig. 3 (b)** in different excitation frequencies. So the frequency is FIP, in which this curve intersects with the X-axis.

#### Results and discussion

In order to investigate the influence that edge characteristic features of detected objects have on the underwater active electrolocation system, two sets of different edge characteristic shapes (cylinder and cuboid, cone and pyramid), whose volumes are little difference in each sets, are carried out in the same materials according

to the way which is presented in the section Methods, respectively. Both the cylinder and cone used in this experiment have an dimension of  $\text{Ø}20\text{ mm} \times 40\text{ mm}$  and the cuboid is  $20\text{ mm} \times 20\text{ mm} \times 40\text{ mm}$ . The pyramid is a tetrahedron whose base is a regular triangle with  $11\text{ mm}$  edges and whose height is  $40\text{ mm}$ . In the experiment, the materials of detected objects are considered as brass, iron, aluminium and plastic, respectively. The excitation of the electrolocation system is set to the  $2\text{ V}$  sine signal with the different frequencies from  $1\text{ Hz}$  to  $1\text{ kHz}$ .

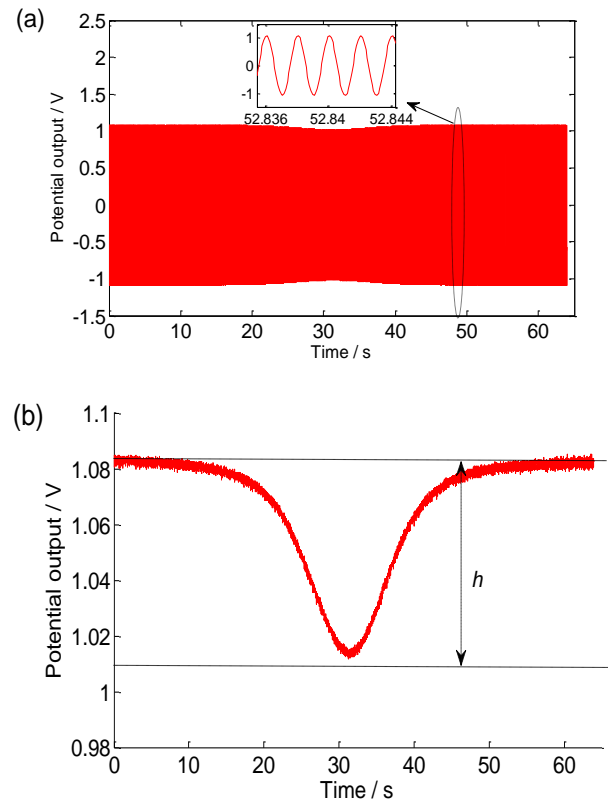


**Fig. 3.** The typical potential output of detection signal.

#### The results based on metal

The HVCs for brass shown in **Fig. 4** can be obtained based on the way proposed in the section Methods and the FIPs of the electrolocation system is intersection of the HVC with the X-axis. As can be observed from these figures, it is illustrated that for the probed object with similar geometric volumes, the FIP of the cuboid is about 50% smaller than the one of the cylinder and the cone is 3.5 times the FIP of the pyramid.

In like manner, the HVCs for iron and aluminium can be gotten, respectively. And their FIPs shown in **Table I** are calculated through the HVCs. Especially, for the iron cuboid, the all amplitude peek in its HVC are less than 0 and there is no the intersection of this curve and the X axis. In addition, the results of the experiment which is carried out in excitations less than  $1\text{ Hz}$  are less precise due to the limitation of the equipment and experimental conditions. So the FIP of the iron cuboid is considered as the less than  $1\text{ Hz}$ .

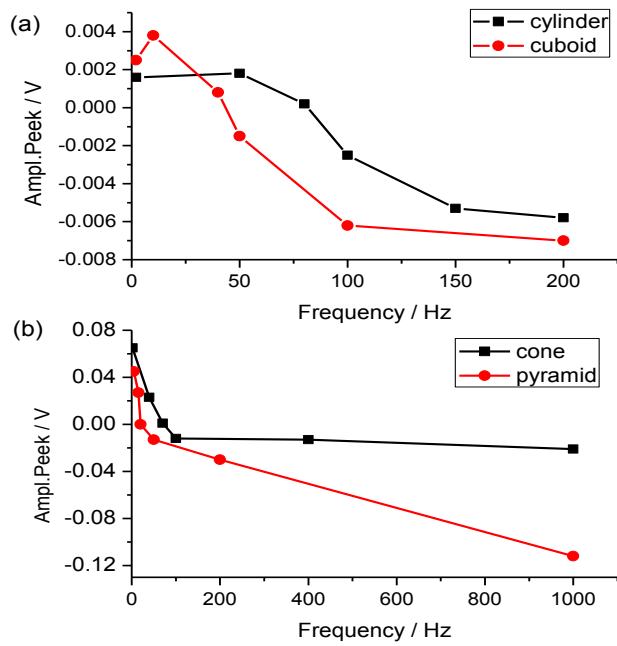


Fig. 4. The HVCs for brass: (a) cylinder and cuboid; (b) cone and pyramid.

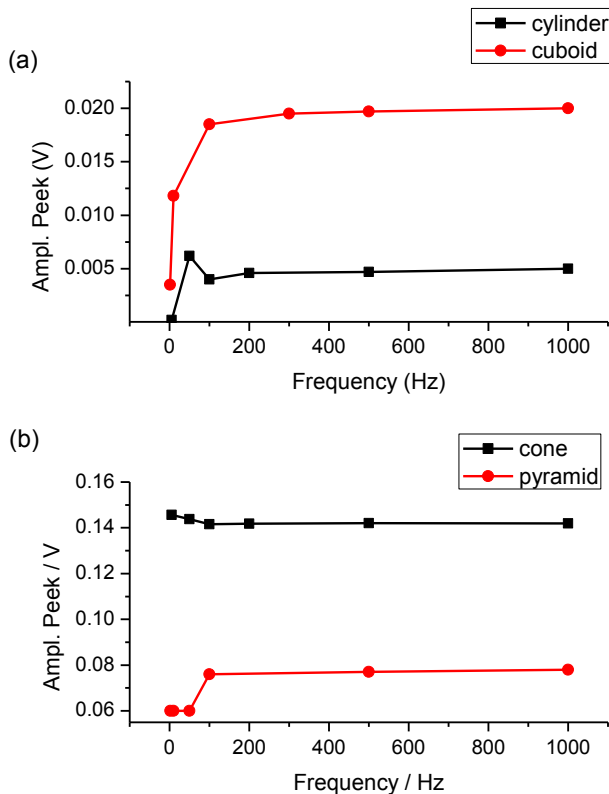


Fig. 5. The HVCs for plastic: (a) cylinder and cuboid; (b) cone and pyramid.

**The results based on plastic**

When the material of probed object is plastic, for the all shapes (cylinder, cuboid, cone, pyramid), the all amplitude peak of the HVCs shown in Fig. 5 are above 0. It is stated that no matter what the shapes of the detected

plastic are, the DFDZ and FIP of AIFC for underwater active electrolocation system is not appear in this case. In other word, any excitation frequency can be used to locate the probed objects.

**Summary**

Based on above all the experiments on AIFC for the objects with different edge characteristics and similar volumes for the underwater active electrolocation system, the summery is shown in Fig. 6 and Table I. In the experiment shown in the section *Methods and Experiment* to explore the influence of the edge characteristics rather than the difference of shapes, we choose the probed objects with similar volume and different edge characteristics, such as cylinder and cuboid whose dimension are  $\varnothing 20 \text{ mm} \times 40 \text{ mm}$  and  $20 \text{ mm} \times 20 \text{ mm} \times 40 \text{ mm}$ , respectively. The volumes of cylinder and cuboid differ very minor, but their edge features are different. By the same token, we choose also the cone and pyramid. As can be observed from the table I, the FIPs for the two sets (cylinder and cuboid, cone and pyramid) are vary widely. Above all, the following results are attained that:

- (1) When the detected objects are plastic, there are no FIPs of AIFC for the underwater active electrolocation system whatever the shapes are.
- (2) For the probed objects are same metallic materials, the different edge characteristics has a great influence on the FIPs of AIFC for the electrolocation system although their volumes are little difference.
- (3) The edge characteristic of probed objects plays an important role in the FIPs of AIFC for the active electrolocation system.

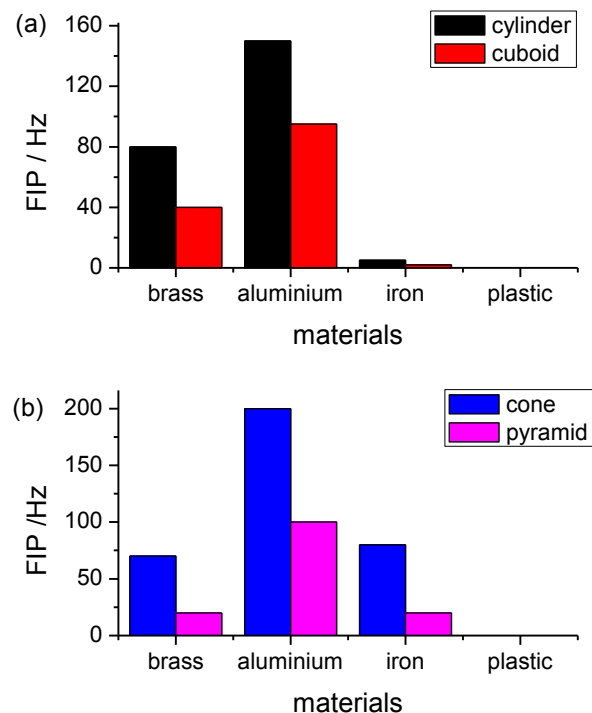


Fig. 6. FIPs for the different edge characteristics with similar volumes.

**Table I.** The FIPs for the different shapes.

Shape	conductor			dielectric
	brass	aluminium	iron	plastic
cylinder	80	150	5	no
cuboid	40	95	< 1	no
cone	70	200	80	no
pyramid	20	100	20	no

\*cylinder:  $\varnothing 20$  mm  $\times$  40 mm; cuboid: 20 mm  $\times$  20 mm  $\times$  40 mm; cone:  $\varnothing 20$  mm  $\times$  40 mm; pyramid: tetrahedron whose base is a regular triangle with 11 mm edges and whose height is 40 mm.

## Conclusion

In this paper, we have investigated the influence that edge features of detected objects have on the underwater active electrolocation system. By analyzing the HVC of different edge characteristic shapes in the same materials, the following conclusions are obtained: (1) for the probed metallic objects with same height and similar geometric volumes similar volumes, for example cylinder and cuboid; or cone and pyramid, their FIPs of AIFC for the underwater active electrolocation system have varied widely. It implied that FIPs are profound associated to the edge characteristics of detected objects of objects; (2) When the detected objects are plastic, the FIPs of AIFC for the electrolocation system have nothing to do with the geometric features of objects, for the FIPs are not reached. At the same time, we found that for the similar geometric features of the probed object, the FIP of the cuboid probed object is about 50% smaller than the FIP of the cylinder probed object. So, the shape of probed object has significant effect on FIP of AIFC for the electrolocation system. In fact, the detail of relationship between AIFC and geometric properties of object is very complicated. So, further study on relationship between probed object shape factor and AIFC is needed. It is impossible for a short passage to resolve completely the issue of the detail of relationship between AIFC and geometric properties of object for electrolocation system. So, further study on relationship between probed object shape factor and AIFC is needed.

## Acknowledgements

This work was supported by the National Natural Science Foundation of China (Grant No. 61573083).

## Supporting information

Supporting informations are available from VBRI Press.

## References

1. Lissmann, H. W.; Machin, K. E. *J. Exp. Biol.* **1958**, 35, 451-486.  
URL: <http://jeb.biologists.org/content/35/2/451>

2. Galizia, C. G.; Lledo, P. M. (Eds.); *Neurosciences-From Molecule to Behavior: A University Textbook*; Heidelberg: Springer, **2013**.  
DOI: [10.1007/978-3-642-10769-6](https://doi.org/10.1007/978-3-642-10769-6)
3. von der Emde G.; Schwarz, S.; Gomez, L.; Budelli, R.; Grant, K. *Nature*, **1998**, 395, 890-894.  
DOI: [10.1038/27655](https://doi.org/10.1038/27655)
4. von der Emde G.; Fetz, S. *J. Exp. Biol.*, **2007**, 210, 3082-3095.  
DOI: [10.1242/jeb.005694](https://doi.org/10.1242/jeb.005694)
5. von der Emde G.; Behr, K.; Bouton, B.; Engelmann, J.; Fetz, S.; Folde, C. *Front Behav. Neurosci.*, **2010**, 4.  
DOI: [10.3389/fnbeh.2010.00026](https://doi.org/10.3389/fnbeh.2010.00026)
6. Rasnow, B. *J. Comp. Physiol. A.*, **1996**, 178, 397-411.  
DOI: [10.1007/BF00193977](https://doi.org/10.1007/BF00193977)
7. Chetty, G.; Russell, A. *2nd Int. Conf. on Bioelectromagnetism*, **1998**, 139-140.  
DOI: [10.1109/ICBEM.1998.666434](https://doi.org/10.1109/ICBEM.1998.666434)
8. Feezor, M. D.; Sorrell, F. Y.; Blankinship, P. R.; Bellingham, J. G. *IEEE J. Oceanic. Eng.*, **2011**, 26, 515-521.  
DOI: [10.1109/48.972086](https://doi.org/10.1109/48.972086)
9. Metzen, M. G.; Biswas, S.; von der Emde, G.; Bousack, H.; Gottwald, M. G.; Mayekar, K. *IEEE Sens. J.*, **2012**, 12, 325-331, 2012.  
DOI: [10.1109/JSEN.2010.2079928](https://doi.org/10.1109/JSEN.2010.2079928)
10. Peng, J. G. *Bioinspiration & Biomimetics*, **2015**, 10, 1-24.  
DOI: [10.1088/1748-3190/10/6/066007](https://doi.org/10.1088/1748-3190/10/6/066007)
11. Yang B.; James S.; Yonatan S. *Intelligent Robots and Systems*, **2012**, 10.  
DOI: [10.1109/IROS.2012.6386174](https://doi.org/10.1109/IROS.2012.6386174)
12. Peng, J. G.; Wu, J. *IEEE Trans. on Appl. Supercond.*, **2016**, 26, 1-4.  
DOI: [10.1109/TASC.2016.2576478](https://doi.org/10.1109/TASC.2016.2576478)
13. Cole, K. S.; Cole, R. H. *J. Chem. Phys.*, **1941**, 9, 341-351.  
DOI: [10.1063/1.1750906](https://doi.org/10.1063/1.1750906)